First-principles calculations for development of low elastic modulus Ti alloys

Hideaki Ikehata, Naoyuki Nagasako, Tadahiko Furuta, Atsuo Fukumoto, Kazutoshi Miwa, and Takashi Saito
Toyota Central Research & Development Laboratories, Inc., Nagakute, Aichi 480-1192, Japan

The elastic constants of the $Ti_{1-x}X_x$ (X=V, Nb, Ta, Mo, and W) and $Zr_{1-x}X_x$ (X=Nb and Mo) binary alloys were calculated for x=0.0, 0.25, 0.5, 0.75, and 1.0 by the ultrasoft pseudopotential method within the generalized gradient approximation to density functional theory to clarify the mechanisms by which the low elastic moduli of the Ti binary alloys are realized. The Young's moduli of the polycrystals for these Ti or Zr binary alloys were calculated from the calculated elastic constants of the single crystal by using the Voigt-Reuss-Hill averaging scheme. The results show that the Young's moduli of the Ti-X or Zr-X binary alloys have the minimum values in the vicinity of x=0.25. From the calculation results, we have found that $C_{11}-C_{12}$ is correlated with the valence electron number per atom and the value of $C_{11}-C_{12}$ becomes nearly zero with the valence electron number of around 4.20–4.24. $C_{11}-C_{12}$ also represents the stability of the bcc structure in these alloys and we thus emphasize that controlling the valence electron number at around 4.20–4.24 is important to realize a low-Young's-modulus material in the Ti or Zr binary alloys having bcc structure.

I. INTRODUCTION

The Ti alloys are well known as light and high-strength materials and have been used in various engineering fields including for the automobile and aerospace applications.[1,2] Recently, Ti alloys have been paid attention as the biomaterials for artificial bones because of their biocompatibility.[3] However, the Young's modulus of a human bone is about 30 GPa, which is much lower than conventional Ti alloys. The difference of Young's moduli between a human bone and an artificial bone causes elastic incompatibility and may harmfully influence healthy bones in the vicinity of the artificial bone. Therefore, not only lightness and high strength but also a low Young's modulus as a human bone is required to the Ti alloys for artificial bones.

It is well known that the addition of Va or VIa family elements such as Nb or V to pure Ti realizes low elastic characteristics (i.e., low Young's modulus).[4] However, the mechanisms of the low elastic moduli have not been clear. If the mechanisms are clarified, the effective materials design for the low elastic characteristic will be available.

Addition of Va family element changes the phase stability of Ti alloys. Although bcc and hcp phases are stable in the Ti-X (X=V, Nb, Ta, Mo, and W) binary alloys, metastable phases such as α' or ω phases should be considered in order to evaluate the Young's moduli of the alloys.[4,5] Especially the ω phase is known to appear in Ti binary alloy containing certain amounts of the Va family element. The ω phase is quite important to discuss (basically it should be avoided) for practical uses of Ti alloys because the existence of the ω phase increases the Young's modulus of the alloy. It is obvious that the ω phase must be avoided to realize low-elastic-modulus alloys as a prerequisite. The amount of metastable phases varies depending on heat treatment conditions and phases without the metastable phases can be obtained by certain heat treatments. Thus we focused on the investigation of elastic moduli of Ti binary alloys having bcc or hcp structures in this research.

From elastic constants $C_{\alpha\beta}$ of a single crystal, Young's modulus of an arbitrary direction in a single crystal can be calculated. However, it is necessary to estimate Young's modulus of a polycrystal from the elastic constants of the single crystal because materials actually used in many cases are polycrystals. We employed the Voigt-Reuss-Hill (VRH) method to evaluate a bulk modulus and a shear modulus of the polycrystal from elastic constants of a single crystal.[6–9]

The elastic constants have been calculated by the first-principles calculations, and it is known that the calculated values agree with the experiments within an accuracy of about ±10%.[10,11] Although differences from the experiment values exist, the elastic constants such as a bulk modulus are reproduced well by these calculations, and it is expected as an effective method to show how to develop a new material whose Young's modulus is controlled. Some examples of calculating the Young's modulus by the VRH method have been reported so far.[12,13] However, a systematic calculation in Ti binary alloys has not been reported yet.

In this research, in order to examine the Young's moduli of Ti binary alloys systematically, we executed the first-principles calculations of the Ti-X (X=V, Nb, Ta, Mo, and W) binary alloys and calculated their elastic constants. Zr-X (X=Nb and Mo) binary alloys were also calculated to find tendencies compared with that in the Ti binary alloys. The Young's modulus was estimated from the calculated elastic constants by the method introduced by Voigt, Reuss, and Hill. From the calculated results, we discuss a guideline to realize low-Young's-modulus materials.

This paper is organized as follows. In Sec. II calculation methods are reviewed. Calculation results to pure metals (V, Nb, Ta, Mo, W, Ti, and Zr) and then to the binary alloys are described in Sec. III. A critical parameter to realize a low-Young's-modulus material is discussed in Sec. IV. Section V concludes this study.

II. METHODS OF CALCULATION

A. Calculation methods of electronic states

The present calculations are performed by the ultrasoft pseudopotential method[14] within generalized gradient ap-

proximation (GGA) to the density functional theory.[15] We adopt the expression proposed by Perdew, Burke, and Ernzerhof[16] for the exchange-correlation energy.

All pseudopotentials are constructed from the results of scalar-relativistic all-electron calculations.[17] The pseudo-wave functions and the pseudoaugmentation charge functions are optimized by the method similar to that proposed by Rappe *et al.*[18]

In constructing the pseudopotentials, $3s$, $3p$, $3d$, $4s$, and $4p$ states are chosen as the reference states for Ti and V atoms. For Zr, Nb, and Mo atoms, $4s$, $4p$, $4d$, $5s$, and $5p$ states and for Ta and W atoms, $5s$, $5p$, $5d$, $6s$, and $6p$ states are chosen as the reference states, respectively. We use double-projector functions for all angular momentum components of all the atoms. The partial core correction[19] is adopted for all pseudopotentials to enhance their transferability.

In the solid-state calculations, the Kohn-Sham equation is solved by the iterative diagonalization scheme[20] and the Broyden charge mixing method[21] is adopted to accelerate the convergence. The macroscopic stress tensor and the atomic forces are utilized for the structural optimization.[22] During the optimization process, the partial occupation numbers near the Fermi level are determined by the Fermi-Dirac distribution function with $k_B T = 3 \times 10^{-3}$ hartree (1 hartree $= 27.2116$ eV) and the free-energy functional[23] is minimized instead of the Kohn-Sham energy functional. The calculations of elastic constants are also performed on the same conditions as mentioned above. On the other hand, in calculating the density of states (DOS), the Kohn-Sham energy functional is minimized with the improved tetrahedron method[24] at the optimized structure. The numbers of **k** points in the irreducible Brillouin zone used for the **k**-space integration are as follows: 195 points for bcc Nb, Ta, Mo, and Ti, 256 points for bcc V and W, 180 points for hcp Ti, 95 points for hcp Zr, 110 points for bcc binary alloys with 1:1 composition, and 72 points for bcc binary alloys with 1:3 or 3:1 compositions.

The pseudowave functions are expanded by plane waves with a cutoff energy equal to 15 hartrees. The cutoff energy for the charge density and potential is set to be 120 hartrees.

B. Calculation of the elastic constants

Elastic constants in a cubic symmetry (C_{11}, C_{12}, and C_{44}) and those in a hexagonal symmetry (C_{11}, C_{12}, C_{13}, C_{33}, and C_{44}) are estimated by calculating the stress tensors on applying minute strains to an equilibrium structure. The amount of the applied strain in the calculation of the stress tensors is about $\pm 1\%$. The linear interpolation scheme was employed in the estimation of the elastic constants from the stresses to remove the residual stress.

C. Estimation of polycrystalline Young's modulus

The Young's modulus of an arbitrary direction can be calculated from elastic constants of a single crystal. However, actual materials industrially used are often polycrystals, treated as isotropic materials. Therefore, to compare a calculation result with experiment, it is necessary to calculate the

value corresponding to the Young's modulus of the polycrystal from the elastic constants of the single crystal. To this end, we utilize the Voigt-Reuss-Hill approximation proposed by Voigt,[6] Reuss,[7] and Hill[8] for averaging the elastic constants of the single crystal.

As shown in Refs. 6–9, once a bulk modulus K_{VRH} and a shear modulus G_{VRH} are obtained by the VRH method, one can calculate the averaged Young's modulus from K_{VRH} and G_{VRH} by the expression

$$E_{VRH} = \frac{9K_{VRH}}{1 + (3K_{VRH}/G_{VRH})}. \tag{1}$$

D. Structure models used in the present calculations

In the calculations of the pure metals, the structures with space group $Im3m$ and $P6_3/mmc$ are assumed for bcc and hcp structures, respectively.

For binary alloys M-X, we selected the chemical compositions $M_{0.75}X_{0.25}$, $M_{0.5}X_{0.5}$, and $M_{0.25}X_{0.75}$. The calculation of the bcc $M_{0.5}X_{0.5}$ binary alloy is performed at the $B2$ structure with the space group $Pm3m$, where the M atom is located on the corner and X atom is located on the body center of the cubic lattice. The primitive brave lattice vectors are $a_1 = (a,0,0)$, $a_2 = (0,a,0)$, and $a_3 = (0,0,a)$. In the calculation of the bcc $M_{0.75}X_{0.25}$ or $M_{0.25}X_{0.75}$ binary alloys, the $D0_3$ structure with space group $Fm3m$ is employed, where the unit cell contains eight conventional bcc unit cells and the primitive brave lattice vectors are $a_1 = (0,a,a)$, $a_2 = (a,0,a)$, and $a_3 = (a,a,0)$, where a is the lattice constant of the conventional bcc unit cell. The atomic positions are $4a(0,0,0)$ site for M atom, $4b\left(\frac{1}{2},\frac{1}{2},\frac{1}{2}\right)$ site for X atom [X(I)], and $8c\left(\frac{1}{4},\frac{1}{4},\frac{1}{4}\right)$ site for two X atoms [X(II)] in $M_{0.25}X_{0.75}$.

The phase diagrams of Ti-X and Zr-X binary alloys have already been researched[25] and it is clear that (a) Ti-X (X = V, Nb, Ta, Mo, and W) binary alloy has a hcp single phase as a stable phase near the pure Ti region at $T=0$ K, (b) a bcc phase is stabilized with an increase of the X element, and (c) finally the bcc single phase becomes stable when the amount of X element is large enough. Although these alloys have other metastable phases to be transformed by a heat treatment such as an α' or ω phase, we assumed that these binary alloys form one of the single phases as mentioned above.

III. RESULTS

A. Pure metals

Tables I and II show the calculation result of the lattice parameters and the elastic constants of bcc metals (V, Nb, Ta, Mo, W) and hcp metals (Ti, Zr), respectively. The calculated lattice parameters show good agreement with experiment within an error normally observed in the GGA. C_{11} and C_{12} of Nb, Ta, Mo, and W are close to the experimental values. All the elastic constants are near the experimental values in Ti and Zr.

Although C_{44}'s of Ta, Mo, and W are within the expected accuracy of $\pm 10\%$ with the experimental values, C_{44}'s of V and Nb show a little difference from the experimental values.

TABLE I. Calculated equilibrium lattice constants a and elastic constants of bcc V, Nb, Ta, Mo, and W. The values of $C_{11}-C_{12}$ are also shown. The experimental values are measured at room temperature.

		a (Å)	C_{11} (GPa)	C_{12} (GPa)	C_{44} (GPa)	$C_{11}-C_{12}$ (GPa)
V	Present	3.004	269.7	139.3	24.9	130.4
	Expt.[a]	3.023	228.7	119.0	43.2	109.7
Nb	Present	3.325	247.0	134.0	15.6	113.0
	Expt.[a]	3.307	246.5	134.5	28.7	112.0
Ta	Present	3.318	257.2	156.1	70.6	101.1
	Expt.[a]	3.298	260.9	157.4	81.8	103.5
Mo	Present	3.169	459.7	161.1	103.8	298.6
	Expt.[a]	3.147	463.0	161.0	109.0	302.0
W	Present	3.187	527.2	192.4	149.0	334.7
	Expt.[a]	3.165	532.6	205.0	163.1	327.6

[a]Reference 26.

However, the differences are only 15–20 GPa and the relative relation of C_{44}'s between these elements are reproduced well by the calculations.

Figure 1 shows the Young's modulus of pure metal polycrystals which were calculated by VRH method from the elastic constants in Tables I and II. The Young's moduli are almost corresponding to the experimental values within the expected accuracy range of ±10%.

The calculations of elastic constants of pure metals with the bcc structure were also performed by Soderlind *et al.* with the full-potential linear muffin-tin orbital (LMTO) method within the local density approximation.[27] Their results also showed an accuracy of about ±10% to the experimental values.

It was clarified that the Young's moduli of the metallic elements by the present method reproduce the experimental values well, and thus we applied the same calculations to their alloys.

B. Young's modulus of the binary alloys

The calculation of the Young's modulus of Ti-*X* binary alloys (*X*=V, Nb, Ta, Mo, and W) and the Zr-*X* (*X*=Nb and Mo) binary alloys has been performed. Table III shows the calculated lattice parameters and elastic constants.

The lattice parameter changes monotonously as the content of *X* increases and it does not show any sudden transitions or local maximal or minimal values.

Figures 2 and 3 show the Young's modulus calculated from the elastic constants in Table III. The Young's moduli lower in all the systems at the 25 at.% contents of a Va or VIa family elements (*X*) and show the minimum values. The Young's moduli increase with increasing the amounts of the *X* elements more than 50 at.%.

Figures 4 and 5 show the calculated DOS's of the Ti-Nb and Ti-Mo binary alloys, respectively. The kind or amount of the *X* element does not seem to affect the shape of DOS but only moves Fermi level. The shift of the Fermi level in Ti-Mo binary system is larger than the one in Ti-Nb binary system at the same content of *X* element, giving that the DOS of $Ti_{0.5}Nb_{0.5}$ resembles that of $Ti_{0.75}Mo_{0.25}$.

IV. DISCUSSION

A. Materials trend of Young's moduli

As shown in Figs. 2 and 3, Young's modulus shows the minimum values at 0.25 at. % of *X* in Ti-*X* and Zr-*X* binary alloys. Then, we investigated whether this phenomenon occurs in other binary systems. Table IV shows additionally calculated compositions and their elastic constants. The Nb-V binary alloy consists of only the Va family elements and the Nb-Mo binary alloy consists of both the Va and VIa family elements. Because the Va and VIa family elements have a bcc structure at 0 K, these alloys were calculated assuming the model of bcc structure same as Ti-*X* and Zr -*X* binary alloys.

On the other hand, $D0_{19}$ structure with the space group $P6_3/mmc$ is assumed in cases of $Ti_{0.75}Zr_{0.25}$ and $Ti_{0.25}Zr_{0.75}$ by consideration of the phase stability of Ti and Zr at 0 K. In this structure, the primitive brave lattice vectors are expressed by $a_1=2a(\sqrt{3}/2,1/2,0)$, $a_2=2a(-\sqrt{3}/2,1/2,0)$, and $a_3=c(0,0,1)$ where a and c correspond to the lattice constants of the conventional hcp unit cell. Two *M* atoms and six *X* atoms are located on the $2c(\frac{1}{3},\frac{2}{3},\frac{1}{4})$ site and $6h(x,2x,\frac{1}{4})$ site, respectively, in the hcp $M_{0.25}X_{0.75}$.

In case of $Ti_{0.5}Zr_{0.5}$, we assumed the lamella structure which has the same unit cell as the conventional hcp unit cell but the Ti and Zr atoms are located on the layer along the *c* axis although this model has the possibility of showing the anisotropy and inaccuracy of the calculation for the elastic constants. The reason for this assumption is to make the

TABLE II. Calculated equilibrium lattice constants a and c and elastic constants of hcp Ti and Zr. The experimental values are measured at room temperature.

		a (Å)	c (Å)	C_{11} (GPa)	C_{12} (GPa)	C_{13} (GPa)	C_{33} (GPa)	C_{44} (GPa)
Ti	Present	2.946	4.666	171.6	86.6	72.6	190.6	41.1
	Expt.[a]	2.951	4.684	162.4	92.0	69.0	180.7	46.7
Zr	Present	3.232	5.182	139.4	71.3	66.3	162.7	25.5
	Expt.[a]	3.231	5.148	143.4	65.3	65.3	164.8	32.0

[a]Reference 26.
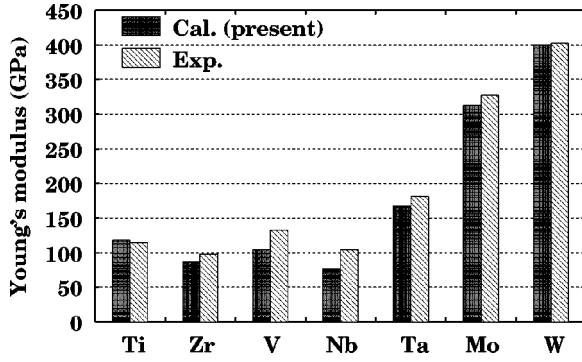
FIG. 1. Young's moduli of hcp metals (Ti and Zr) and bcc metals (V, Nb, Ta, Mo, and W) estimated from the calculated elastic constants of the single crystal by the Voigt-Reuss-Hill method. Experimental Young's moduli are measured values for polycrystalline metals at room temperature (Ref. 26).

calculation time reduced. Moreover, the Ti-Nb binary alloy was calculated with the hcp structures to compare with the result of the bcc structure.

The obtained lattice parameters and elastic constants are shown in Tables IV and V for the bcc Nb-X (X=V and Mo) binary alloys and the hcp Ti-X (X=Zr and Nb) binary alloy, respectively, and the results of the Young's moduli calculated by Eq. (1) are shown in Fig. 6. In any case, the rapid transition of the Young's modulus with the minimum value such as shown in Figs. 2 and 3 was not observed and the Young's

modulus monotonically increases or decreases with the content of X.

The result of Ti$_{0.5}$Zr$_{0.5}$ which does not show an extreme change of neither the lattice parameter nor the Young's modulus indicates the validity of the model used for this composition. When the content of Nb is 50 at. % or more in Ti-Nb binary system having hcp structure, the C_{44} becomes negative. It means addition of 50 at. % or more Nb makes hcp structure unstable in Ti-Nb binary system. These results agree with the experimental phase diagram of Ti-Nb binary system, where the hcp phase becomes unstable in Ti$_{0.5}$Nb$_{0.5}$ (Ref. 25). On the other hand, in Ti$_{0.75}$Nb$_{0.25}$, though the value of C_{44} is very small, the conditions $C_{11} > |C_{12}|$, $C_{33}(C_{11} + C_{12}) > 2C_{13}^2$, $C_{11}C_{33} > C_{13}^2$, and $C_{44} > 0$, which represent elastic stability of the hcp structure, are satisfied.

Moreover, in paying attention to Ti$_{0.75}$Nb$_{0.25}$, Young's modulus is 31 GPa for the bcc structure, which is lower than 62 GPa for the hcp structure. This result suggests that the bcc is more preferred structure for lowering Young's modulus.

It turns out that the change in the Young's moduli shown in Figs. 2 and 3 is observed only when the binary alloy consists of both the IVa family element and the Va or VIa family element. It is obvious from their phase diagrams that the phase transition between hcp and bcc structure is involved in the binary systems.[25]

B. Phase stability of the bcc structure

Although pure Ti and Zr have the hcp structure (α phase) at room temperature, they transform into the bcc structure (β

TABLE III. Calculated equilibrium lattice constants a, elastic constants C_{11}, C_{12}, and C_{44}, and $C_{11} - C_{12}$ of bcc Ti-X (X=V, Nb, Ta, Mo, and W) Zr-Nb, and Zr-Mo binary alloys.

Composition $M_{1-x}X_x$	Structure	a (Å)	C_{11} (GPa)	C_{12} (GPa)	C_{44} (GPa)	$C_{11} - C_{12}$ (GPa)
Ti$_{0.75}$V$_{0.25}$	$D0_3$	3.273	123.9	116.9	36.3	7.0
Ti$_{0.5}$V$_{0.5}$	$B2$	3.280	169.6	122.3	33.6	47.3
Ti$_{0.25}$V$_{0.75}$	$D0_3$	3.306	213.0	132.2	29.6	80.8
Ti$_{0.75}$Nb$_{0.25}$	$D0_3$	3.273	128.5	115.5	14.9	13.0
Ti$_{0.5}$Nb$_{0.5}$	$B2$	3.280	155.4	124.7	12.8	30.7
Ti$_{0.25}$Nb$_{0.75}$	$D0_3$	3.306	203.5	126.8	21.3	76.8
Ti$_{0.75}$Ta$_{0.25}$	$D0_3$	3.271	129.9	121.6	38.6	8.2
Ti$_{0.5}$Ta$_{0.5}$	$B2$	3.278	163.4	132.8	39.0	30.6
Ti$_{0.25}$Ta$_{0.75}$	$D0_3$	3.302	207.0	145.3	55.6	61.7
Ti$_{0.75}$Mo$_{0.25}$	$D0_3$	3.273	160.5	125.6	34.1	34.8
Ti$_{0.5}$Mo$_{0.5}$	$B2$	3.280	224.0	146.6	10.4	77.5
Ti$_{0.25}$Mo$_{0.75}$	$D0_3$	3.306	363.6	151.5	62.0	212.2
Ti$_{0.75}$W$_{0.25}$	$D0_3$	3.217	169.2	134.2	32.4	35.0
Ti$_{0.5}$W$_{0.5}$	$B2$	3.184	239.9	165.9	50.9	73.9
Ti$_{0.25}$W$_{0.75}$	$D0_3$	3.179	374.8	184.2	81.7	190.6
Zr$_{0.75}$Nb$_{0.25}$	$D0_3$	3.508	112.8	98.3	19.8	14.5
Zr$_{0.5}$Nb$_{0.5}$	$B2$	3.447	144.4	108.3	18.3	36.1
Zr$_{0.25}$Nb$_{0.75}$	$D0_3$	3.382	196.2	118.5	17.9	77.7
Zr$_{0.75}$Mo$_{0.25}$	$D0_3$	3.451	138.4	104.2	16.6	34.2
Zr$_{0.5}$Mo$_{0.5}$	$B2$	3.349	208.5	124.3	29.2	84.2
Zr$_{0.25}$Mo$_{0.75}$	$D0_3$	3.244	342.4	134.5	49.7	207.9
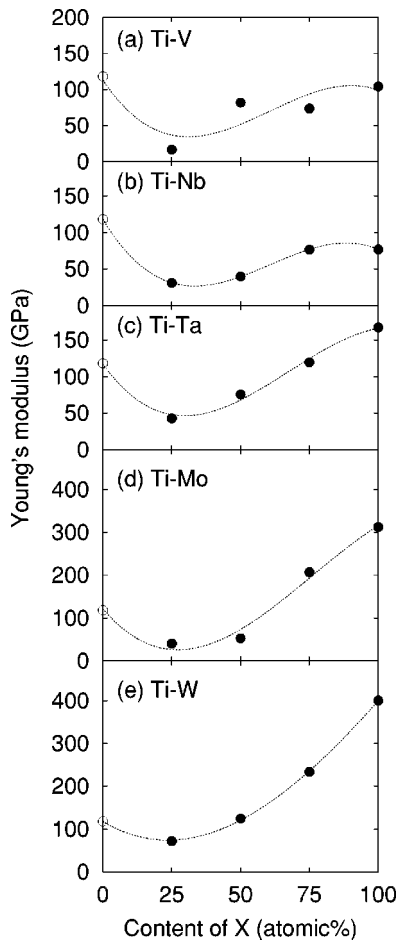
FIG. 2. Young's moduli estimated from the calculated elastic constants of the single crystals by the Voigt-Reuss-Hill method. Solid circles are calculated values for bcc Ti-X binary alloys (X =V, Nb, Ta, Mo, and W). Open circles are the calculated Young's modulus of hcp Ti. Dotted lines denote the curve fitted by third-order polynomial function which is shown as a guide to the eye.
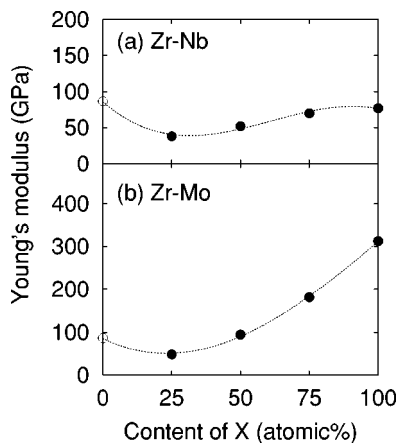
FIG. 3. Young's moduli estimated from the calculated elastic constants of the single crystals by the Voigt-Reuss-Hill method. Solid circles are calculated values for bcc Zr-X binary alloys (X =Nb and Mo). Open circles are the calculated Young's modulus of hcp Zr. Dotted lines denote the curve fitted by a third-order polynomial function which is shown as a guide to the eye.
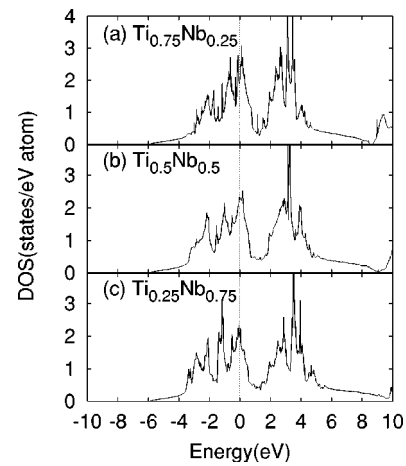
FIG. 4. Calculated total density of states (DOS) of bcc Ti-Nb binary alloys: (a) $Ti_{0.25}Nb_{0.75}$, (b) $Ti_{0.5}Nb_{0.5}$, and (c) $Ti_{0.75}Nb_{0.25}$. A vertical dotted line denotes the Fermi energy.

phase) at about 1155 K and 1136 K, respectively. Then elastic properties of β-Ti and β-Zr were calculated although T =0 K is assumed in the calculations. The elastic constants are shown in Table VI, which show good agreement with the result by Ahuja *et al.*[28]

Young's modulus in the $\langle 001 \rangle$ direction, E_{001}, is expressed by

$$E_{001} = \frac{(C_{11}+2C_{12})(C_{11}-C_{12})}{C_{11}+C_{12}}. \quad (2)$$

The calculated E_{001}'s for β-Ti and β-Zr are the negative values -38 GPa and -11 GPa, respectively. This result means that Ti and Zr of the bcc structure cannot exist stably at absolute zero. This is in good agreement with actual phase stability. It is clear that E_{001} becomes negative only when $C_{11}-C_{12}$ becomes negative from Eq. (2). The $C_{11}-C_{12}$ is negative only for β-Ti and β-Zr as shown in Table VI and positive for the Va and VIa family elements and the binary systems with the bcc structure from Tables I, III, and IV. The
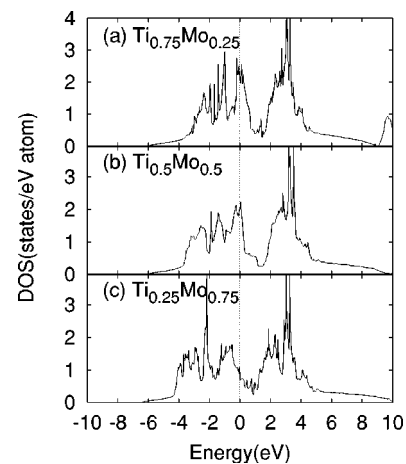
FIG. 5. Calculated total density of states (DOS) of bcc Ti-Mo binary alloys: (a) $Ti_{0.25}Mo_{0.75}$, (b) $Ti_{0.5}Mo_{0.5}$, and (c) $Ti_{0.75}Mo_{0.25}$. A vertical dotted line denotes the Fermi energy.

TABLE IV. Calculated equilibrium lattice constants a, elastic constants C_{11}, C_{12}, and C_{44}, and $C_{11}-C_{12}$ of bcc Nb-V and Nb-Mo binary alloys.

Composition $Nb_{1-x}X_x$	Structure	a (Å)	C_{11} (GPa)	C_{12} (GPa)	C_{44} (GPa)	$C_{11}-C_{12}$ (GPa)
$Nb_{0.75}V_{0.25}$	$D0_3$	3.256	244.6	135.9	16.5	108.7
$Nb_{0.5}V_{0.5}$	B_2	3.177	250.3	136.1	12.3	114.3
$Nb_{0.25}V_{0.75}$	$D0_3$	3.094	252.2	137.2	17.0	115.0
$Nb_{0.75}Mo_{0.25}$	$D0_3$	3.279	286.8	143.5	23.8	143.3
$Nb_{0.5}Mo_{0.5}$	B_2	3.238	368.4	140.7	63.3	227.7
$Nb_{0.25}Mo_{0.75}$	$D0_3$	3.202	425.5	144.8	85.4	280.7

value of $C_{11}-C_{12}$ is the parameter by which the elastic stability of a bcc structure can be evaluated[29] and it is necessary to become positive for the bcc structure stabilization.

C. Relationship between the elastic constants C_{11} and C_{12} and the number of valence electrons

The change in the Young's modulus does not depend so much on the kind of IVa, Va, and VIa family elements as seen in Figs. 2 and 3. Moreover, the shapes of the DOS do not depend on the kind of the elements but the crystal structures as discussed by Söderlind *et al.*[27] This tendency of the DOS is seen not only for pure metals but also for binary alloys. The DOS resemble each other very well when they have the same crystal structure as shown in Figs. 4 and 5. Thus the rigid band model can be applied, where the position of Fermi level corresponding to the valence electron number per atom is a parameter to describe the elastic characteristics of the alloys.

It is evident that in the cubic symmetry the Young's modulus is lowered by making $C_{11}-C_{12}$ and C_{44} smaller.[9] Figure 7 shows the relationship between the valence electron number per atom for Ti-X and Zr-X binary alloys and elastic constants C_{11} and C_{12} in the bcc structures. It is clear that both C_{11} and C_{12} increase monotonically with increasing the valence electron number per atom. $C_{11}-C_{12}$ also shows the same tendency as shown in Fig. 8. Moreover, by plotting the calculation values of β-Ti and β-Zr to Fig. 8, it is obvious that $C_{11}-C_{12}$ shows an almost linear dependence with the valence electron number from 4 to 6. Figure 8 shows that $C_{11}-C_{12}$ takes a value close to zero around the valence electron number of 4.20–4.24.

The bcc structures thus cannot exist stably in the area of a valence electron number less than 4.20, where $C_{11}-C_{12}$ becomes negative. In other words, the bcc structure of the valence electron number around 4.20–4.24 realizes a small $C_{11}-C_{12}$ and thereby a low Young's modulus is expected if bcc structure can be maintained.

On the other hand, as the stability of the hcp structure increases with decreasing the valence electron number from 4.24, it tends to be difficult to stabilize the bcc single-phase structure even if $C_{11}-C_{12}$ is still positive. In this case the hcp structure or metastable phases such as the ω phase can be formed and it is obvious that the existence of these phases causes an increase of Young's modulus.[4] Therefore, it is necessary to choose a proper composition and process to stabilize the bcc structure.

D. Relationship between C_{44} and the number of valence electrons

Figure 9 shows the relationship between the valence electron number and C_{44} of the Ti-X binary alloys and the pure metals. The plots are scattered and the relation with the valence electron number is not clear. It seems that C_{44}'s are determined not only the valence electron number per atom but also the other parameters.

It is obvious that C_{44}'s of the binary alloys whose X element has small C_{44} were kept small—e.g., Ti-Nb from Tables I–IV. It is assumed that addition of the element having small C_{44} is better for lowering C_{44} of the alloys.

E. Conditions for low elastic modulus and applications

From the discussions mentioned above, using the binary alloy which consists of a IVa family element and a Va or VIa

TABLE V. Calculated equilibrium lattice constants a and c and elastic constants C_{11}, C_{12}, C_{13}, C_{33}, and C_{44} of hcp Ti-Zr and Ti-Nb binary alloys. In the hexagonal symmetry, $C_{66}=\frac{1}{2}(C_{11}-C_{12})$.

Composition $Ti_{1-x}X_x$	Structure	a (Å)	c (Å)	C_{11} (GPa)	C_{33} (GPa)	C_{12} (GPa)	C_{13} (GPa)	C_{44} (GPa)
$Ti_{0.75}Zr_{0.25}$	$D0_{19}$	3.036	4.772	140.4	172.8	87.5	72.4	35.3
$Ti_{0.5}Zr_{0.5}$	Lamella	3.114	4.918	137.7	164.0	75.3	67.8	30.0
$Ti_{0.25}Zr_{0.75}$	$D0_{19}$	3.172	5.049	136.1	159.0	77.1	69.8	29.9
$Ti_{0.75}Nb_{0.25}$	$D0_3$	2.930	4.783	207.1	187.4	58.1	96.6	1.9
$Ti_{0.5}Nb_{0.5}$	Lamella	2.915	4.859	266.8	257.2	45.0	107.0	-7.1
$Ti_{0.25}Nb_{0.75}$	$D0_{19}$	2.875	5.162	232.8	215.1	111.4	108.7	-33.9
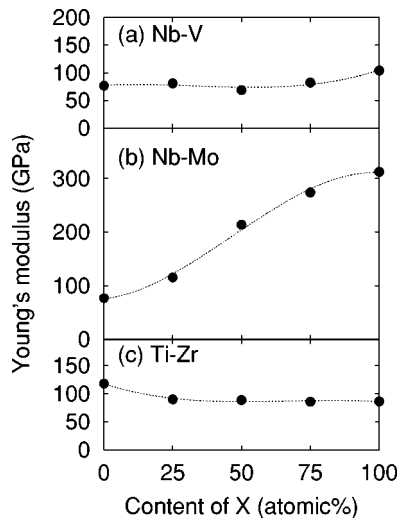
FIG. 6. Young's moduli estimated from the calculated elastic constants of the single crystals by the Voigt-Reuss-Hill method for (a) bcc Nb-V, (b) bcc Nb-Mo, and (c) hcp Ti-Zr. Dotted lines denote the curve fitted by a third-order polynomial function which is shown as a guide to the eye.

family element, a low Young's modulus can be achieved by meeting the following requirements at the same time: (1) By adding the Va or VIa element which stabilizes the bcc structure to the IVa element which has stable hcp structure at $T=0$ K, the valence electron number is controlled to be around 4.20–4.24 to make the value of $C_{11}-C_{12}$ nearly zero, and simultaneously it should maintain the bcc structure. (2) C_{44} of the binary alloy is small.

For instance, in case of the Ti-Nb binary alloy, the valence electron number per atom becomes 4.24 by adding 24 at.% Nb, and then $C_{11}-C_{12}$ becomes almost zero. Moreover, it is expected that C_{44} of the composition becomes lower because Nb has a low C_{44} value. Although $Ti_{0.76}Nb_{0.24}$ is usually expected to be the hcp structure at absolute zero, it is possible to obtain bcc single-phase structure by an appropriate heat treatment. On the other hand, in $Ti_{0.8}Nb_{0.2}$, the valence electron number becomes 4.20 where the lower $C_{11}-C_{12}$ is expected, but the bcc structure tends to be unstabilized more and not only the hcp structure but also the metastable phases are expected to appear. Therefore realizing the bcc single phase at absolute zero becomes more difficult for the composition.

Because the relationship between $C_{11}-C_{12}$ and the valence electron number per atom does not depend on the kind of the additional element, a similar situation can be expected in alloy systems with three or more elements if the compo-

TABLE VI. Calculated equilibrium lattice constants and elastic constants of β-Ti and β-Zr.

	a (Å)	C_{11} (GPa)	C_{12} (GPa)	C_{44} (GPa)	$C_{11}-C_{12}$ (GPa)
β-Ti	3.264	87.8	112.2	39.8	−24.4
β-Zr	3.580	84.2	91.4	32.3	−7.2
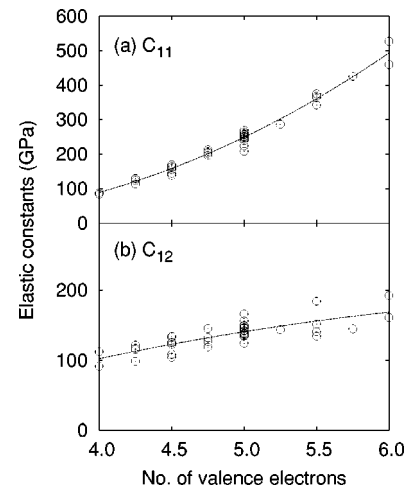
FIG. 7. Calculated elastic constants (a) C_{11} and (b) C_{12} of the Ti and Zr binary alloys and pure metals. The values at valence electron number of 4.0 are of bcc Ti and Zr.

sitions belong to IVa–VIa family. The composition of the recently developed material named "GUM METAL," which realized an extreme low Young's modulus and high strength at the same time, is Ti-12Ta-9Nb-3V-6Zr-O and Ti-23Nb-0.7Ta-2Zr-O (mol %), for example.[30,31] Both are bcc single-phase Ti alloys designed so that each valence electron number becomes about 4.22–4.24.[30,31] Because a lot of Nb which is added to this alloy is the element with low C_{44}, these alloys prove the above conditions of a low-Young's-modulus alloy.

V. CONCLUSIONS

We performed the first-principles calculations of the Young's moduli of $Ti_{1-x}X_x$ (X=V, Nb, Mo, and W) and $Zr_{1-x}X_x$ (X=Nb and Mo) binary alloys for x=0.0, 0.25, 0.5, 0.75, and 1.0 by means of the Voigt-Reuss-Hill averaging scheme. The calculated Young's moduli have minimum values at some content of additional X atoms.

By analyzing the calculated results, we have confirmed that the electronic structure of these bcc alloys are mainly determined by their crystal structure—that is, the so-called rigid band model is able to be applicable and the influence of the individual elements is not so dominant. In fact, the cal-
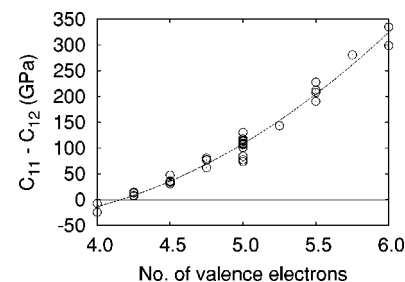
FIG. 8. Calculated values of $C_{11}-C_{12}$ of the Ti and Zr binary alloys and pure metals. The values at valence electron number of 4.0 are of bcc Ti and Zr.
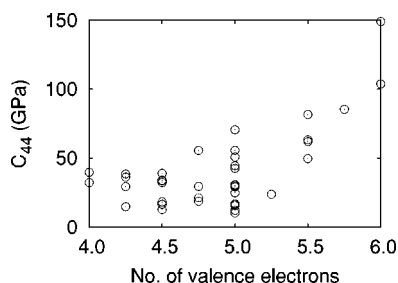
FIG. 9. Calculated values of C_{44} of the Ti and Zr binary alloys and pure metals. The values at valence electron number of 4.0 are of bcc Ti and Zr.

culated C_{11} and C_{12} has good correlation with the valence electron number per atom as expected from the rigid band model. It was also confirmed that $C_{11}-C_{12}$ is nearly zero at the valence electron number per atom of around 4.20–4.24.

From the calculated results, we consider that the low elastic moduli in the β-Ti alloys are established by two fac-

tors: (1) The valence electron number per atom of Ti binary alloy can be controlled by the amount of Va or VIa family element such as Nb and Ta, resulting in $C_{11}-C_{12}$ being nearly zero. (2) The bcc structure is maintained. On the other hand, it is not clear from the present study that there are any factors which can describe the behavior of C_{44}.

It is confirmed that the recently developed super-low-elastic Ti alloy named "GUM METAL" satisfied the condition that the valance electron number per atom is around 4.24 and $C_{11}-C_{12}$ is expected to be nearly zero. The compositions of GUM METAL are optimized according to the prescription obtained from the present calculation.

ACKNOWLEDGMENTS

[1] T. Yamaguchi, H. Morishita, S. Iwase, S. Yamada, T. Furuta, and T. Saito, SAE Trans. J. Mater. Manuf. **109**, 416 (2000).

[2] P. J. Winkler, M. A. Daubler, and M. Peters, in *Titanium '92 Science and Technology: Proceedings of a Symposium Sponsored by the Titanium Committee of Minerals, Metals & Materials Structural*, edited by F. H. Froes and I. L. Caplan (tms, 1993), p. 2877.

[3] D. Kuroda, M. Niinomi, M. Morinaga, Y. Kato, and T. Yashiro, Mater. Sci. Eng., A **243**, 244 (1998).

[4] S. G. Fedotov, in *Titanium Science and Technology: Proceedings of the 2nd International Conference*, edited by R. I. Jaffee and H. M. Burte (Plenum Press, New York, 1973), p. 871.

[5] N. Sakaguchi, M. Niinomi, T. Akahori, T. Saito, and T. Furuta, J. Jpn. Inst. Met. **67**, 681 (2003).

[6] W. Voigt, *Lehrbuch der Kristallphysik* (Teubner, Leipzig, 1928), pp. 716–761.

[7] A. Reuss, Z. Angew. Math. Mech. **9**, 49 (1929).

[8] R. Hill, Proc. Phys. Soc., London, Sect. A **65**, 349 (1952).

[9] G. Grimvall, *Thermophysical Properties of Materials* (North-Holland, Amsterdam, 1999).

[10] G. Y. Guo and H. H. Wang, Phys. Rev. B **62**, 5136 (2000).

[11] P. T. Jochym and K. Parlinski, Phys. Rev. B **65**, 024106 (2001).

[12] Y. Lee and B. N. Harmon, J. Alloys Compd. **338**, 242 (2002).

[13] K. Chen and L. R. Zhao, J. Appl. Phys. **93**, 2414 (2003).

[14] D. Vanderbilt, Phys. Rev. B **41**, 7892 (1990); K. Laasonen, A. Pasquarello, R. Car, C. Lee, and D. Vanderbilt, *ibid.* **47**, 10 142 (1993).

[15] P. Hohenberg and W. Kohn, Phys. Rev. **136**, B864 (1964); W. Kohn and L. J. Sham, Phys. Rev. **140**, A1133 (1965).

[16] J. P. Perdew, K. Burke, and M. Ernzerhof, Phys. Rev. Lett. **77**, 3865 (1996); **78**, 1396(E) (1997).

[17] D. D. Koelling and B. N. Harmon, J. Phys. C **10**, 3107 (1977).

[18] A. M. Rappe, K. M. Rabe, E. Kaxiras, and J. D. Joannopoulos, Phys. Rev. B **41**, 1227 (1990).

[19] S. G. Louie, S. Froyen, and M. L. Cohen, Phys. Rev. B **26**, 1738 (1982).

[20] M. P. Teter, M. C. Payne, and D. C. Allen, Phys. Rev. B **40**, 12 255 (1989).

[21] V. Eyret, J. Comput. Phys. **123**, 271 (1996).

[22] N. Ohba, K. Miwa, N. Nagasako, and A. Fukumoto, Phys. Rev. B **63**, 115207 (2001).

[23] N. D. Mermin, Phys. Rev. **137**, A1141 (1965).

[24] P. E. Blöchl, O. Jepsen, and O. K. Andersen, Phys. Rev. B **49**, 16 223 (1994).

[25] B. Hugh, *Alloy Phase Diagrams* (ASM, 1992).

[26] *Metals, Thermal and Mechanical Data*, Vol. 16 of *International Tables of Selected Constants*, edited by S. Allard (Pergamon Press, New York, 1969).

[27] P. Söderlind, O. Eriksson, J. M. Wills, and A. M. Boring, Phys. Rev. B **48**, 5844 (1993).

[28] R. Ahuja, J. M. Wills, B. Johansson, and O. Eriksson, Phys. Rev. B **48**, 16 269 (1993).

[29] G. V. Sin'ko and N. A. Smirnov, J. Phys.: Condens. Matter **14**, 6989 (2002).

[30] T. Saito, T. Furuta, J. Hwang, S. Kuramoto, K. Nishino, N. Suzuki, R. Chen, A. Yamada, K. Ito, Y. Seno, T. Nonaka, H. Ikehata, N. Nagasako, C. Iwamoto, Y. Ikuhara, and T. Sakuma, Science **300**, 464 (2003).

[31] T. Furuta, K. Nishino, J. H. Hwang, K. Ito, S. Osawa, S. Kuramoto, N. Suzuki, R. Chen, and T. Saito, in *Ti-2003 Science and Technology: Proceedings of 10th World Conference on Titanium*, edited by G. Luetjering and J. Albrecht (Wiley, Europe, 2004), p. 1519.